BLUFF-BODY AERODYNAMICS AND FREE-STREAM TURBULENCE IN PRECIPITATION MEASUREMENTS

Arianna Cauteruccio [1,2*], Matteo Colli [3] & Luca G. Lanza [1,2]

(1) Department of Civil, Chemical and Environmental Engineering, University of Genova, Genoa, Italy
(2) WMO/CIMO Lead Centre "B. Castelli" on Precipitation Intensity, Italy
(3) Artys srl, Genoa, Italy

**email: arianna.cauteruccio@edu.unige.it*

KEY POINTS

- *Wind is turbulent in nature and precipitation gauges are immersed in a turbulent flow*
- *Free-stream turbulence intensity is obtained from high frequency 3-D sonic anemometer data*
- *Large Eddy Simulations both in uniform and turbulent free-stream conditions are performed*
- *The free-stream turbulence effect is quantified by computing the gauge's Collection Efficiency*

1 INTRODUCTION

The numerical studies reported in the literature about the wind-induced biases of precipitation measurements, assume that turbulence is only generated by the bluff-body aerodynamic of precipitation gauge with the obstruction to the airflow inducing updraft velocity components, airflow acceleration and development of turbulent fluctuations. Therefore, Computational Fluid Dynamics (CFD) simulations are generally performed under steady and uniform incoming airflow conditions. *Nešpor & Sevruk* (1999) conducted numerical simulations on three cylindrical gauges with different size and varying the shape of the collector rim. The aerodynamic response of each gauge was calculated using a time average approach based on a turbulence closure model, and then liquid particle trajectories were computed to assess the gauge collection performances. A one-way coupled model, which neglects the interaction between particles and the effect of the particles on the air was employed. This model separately simulates spherical particles for each diameter and the Collection Efficiency (CE) is calculated as the integral, over the particle size distribution, of the number of particles collected by the gauge with respect to the total precipitation. This simulation scheme was adopted also by *Thériault et al.* (2012) and *Colli et al.* (2015, 2016a, 2016b) for solid precipitation, by increasing the details of the computational mesh to better capture the airflow features. In the work of *Thériault et al.* (2012) different crystal types were modelled by using a power law parametrization of the terminal velocity, volume, density and cross section of the particles, while in the work of *Colli et al.* (2016b) two macro categories were modelled: wet and dry snow. A fixed drag coefficient for each crystal type was adopted and results were compared with field measurements in terms of collection efficiency. The obtained CE curves for the two macro categories act as upper and lower thresholds of the wide spreading of experimental data. *Colli et al.* (2015) obtained a better fit of the collection efficiency curves with real-world data, calculating the snowflake trajectories by updating the Reynolds number and the associated drag coefficient at each time step.

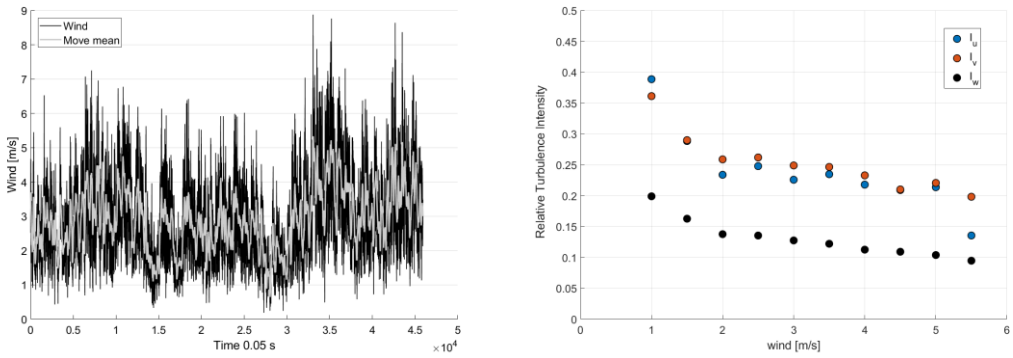

Figure 1 High-frequency wind measurements from the Nafferton site (black line) and moving average with N=125 (grey line) in the left-hand panel and relative turbulence intensity for the three Cartesian directions for each wind class in the right-hand panel.

Wind is turbulent in nature due to the roughness of the site and the presence of obstacles; therefore, in operational conditions precipitation gauges are immersed in a turbulent flow. In the work of *Cauteruccio et al.* (2019) the free-stream turbulence effect on the airflow fields around an inverted-conical shaped gauge was quantified, by means of both CFD simulations and wind tunnel tests, based on the comparison between the aerodynamic response of the gauge under uniform and turbulent free-stream conditions. Results showed that the normalized updraft, downdraft and airflow acceleration above the gauge collector are less accentuated in the turbulent free-stream configuration than in uniform free-stream conditions due to the energy dissipation induced by turbulent fluctuations. This observed damping effect is consistent with the work of *Colli et al.* (2015), where a general overestimation of the wind-induced error when performing simulations under steady-uniform free-stream conditions was evident from the comparison with field observations.

In the present work, further to the role of the local generation of turbulence due to the obstruction to the airflow caused by the bluff body nature of the precipitation gauge, the natural free-stream turbulence inherent to the wind, and its influence on precipitation measurements, are further investigated.

2 METHODOLOGY

In the present work, the wind-induced bias on precipitation measurements, due to the aerodynamic response of a chimney-shaped gauge when impacted by wind and to the free-stream turbulence inherent to the natural airflow, is addressed by means of a numerical approach. Large Eddy Simulations (LES), both in uniform and turbulent free-stream conditions, were performed to obtain the airflow features around the gauge. With the aim to simulate turbulence intensity values characterizing the wind near to the ground surface, 3-D high-frequency (20 Hz) sonic anemometer measurements from the Nafferton (UK) experimental site were analyzed. In the simulation, the free-stream turbulence was generated by introducing geometrical obstacles upstream of the gauge and their distance from the gauge, along the longitudinal direction, was calibrated to obtain the desired level of turbulence intensity, as measured in the Nafferton site. Subsequently, catch ratios for dry snow particles were obtained by running a literature Lagrangian Particle Tracking model (*Colli et al.*, 2015) applied to the LES airflow fields and collection efficiency values were calculated as the integral over the full range of particle diameters after assuming a suitable Particle Size Distribution (PSD) for the precipitation process. Results are reported in terms of a comparison between catch ratios and collection efficiency values calculated for the two free-stream turbulence conditions.

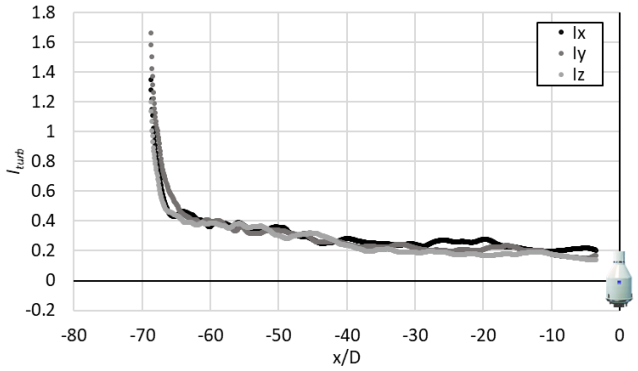

Figure 2 Decrease of the three numerical relative turbulence intensity profiles at the gauge collector elevation (z/D = 0) along the spatial domain between the position of the columnar obstacles (x/D = -70) and the gauge position (x/D = 0).

3 RESULTS AND DISCUSSION

3.1 The free-stream turbulence in natural wind

In the literature, various studies (e.g. *Øistad*, 2015) report estimates of the free-stream turbulence intensity mainly at high elevation (70-100 m). For this reason, in this work, 38 minutes of high-frequency (20 Hz) wind measurements at the gauge elevation from the Nafferton (UK) experimental site, kindly provided by Environmental Measurements Ltd. (EML) (see Figure 1, black line, left-hand panel), were analyzed. The

moving average (Figure 1, grey line, left-hand panel) was calculated by testing different sizes (N) for the moving window using a try and error procedure. A value of N=125 was chosen because of its consistency with the average approach proposed by Reynolds which requires that the mean values of the turbulent fluctuations in all directions (x, y, z) must be null. The wind measurements were divided in wind classes based on the mean values of their average magnitude and the relative turbulence intensity value in each direction and for each wind class were calculated (Figure 1 right-hand panel). The obtained turbulence intensity values along the two longitudinal directions (x and y) are similar for each wind speed class, while they are lower for the vertical direction (z). As shown in the literature for high elevation measurements, even close to the ground, the turbulence intensity decreases with increasing the wind speed and seems to have an asymptotical constant limit.

3.2 Numerical generation of free-stream turbulence for the chimney-shaped gauge

The free-stream turbulence effect was investigated by performing CFD simulations on a catching type precipitation gauge, the GeonorT200B©, characterized by the typical chimney shape of weighing gauges. For the two free-stream conditions, simulations were performed by imposing a wind speed equal to U_{ref} = 6 ms^{-1} at the inlet surface of the computational domain (upwind y, z plane) as a boundary condition. The free-stream turbulence was generated by introducing three columnar obstacles upstream of the gauge and LES were chosen in order to ensure a good development of the turbulence wake downwind to the obstacles before impacting on the gauge surface. When the airflow overtakes the three obstacles its mean velocity magnitude is decelerated and assumes the value of 2.5 ms^{-1}, which becomes the new reference wind speed (U_{ref}) for the turbulent free-stream configuration. The decay along the longitudinal direction (x/D) of the three relative turbulence intensity profiles at the gauge collector elevation (z/D = 0) is shown in Figure 2. The distance (x/D = -70) between the position of the columnar obstacles and the precipitation gauge was calibrated in order to obtain, for the reference wind speed, the level of turbulence measured at the Nafferton site. A very fine computational mesh was realized, for instance the surface of the collector rim was discretized with 0.35 mm cells. Refinement boxes were realized around the gauge, and the surface of the gauge body was discretized with a gradually increasing mesh while approaching the gauge surface (Figure 3). In turbulent free-stream conditions the computational mesh around the three columnar obstacles with size 0.3 x 0.3 x 7 m was refined, and this produced an increase of the computational burden. The three columnar obstacles are spaced by 0.3 m and extend four meters above and three meters below the elevation of the gauge collector. The computational mesh for the simulation under uniform free-stream conditions is composed by twelve million cells, while by introducing the three columnar obstacles the number of cells reached fourteen million. Sample simulation results are reported in Figure 4 where the normalized magnitude of the instantaneous (t = 22.5 s) flow velocity in the horizontal plane (x,y) at the gauge collector elevation (z/D=0) and the normalized vertical component (U_z/U_{ref}) in the vertical plane (x,z) at y/D=0 are reported for the turbulent free-stream conditions. This picture shows that the gauge collector is totally immersed in the turbulent flow generated by the three obstacles while in the transversal direction the flow field starts to become uniform many diameters away from the collector.

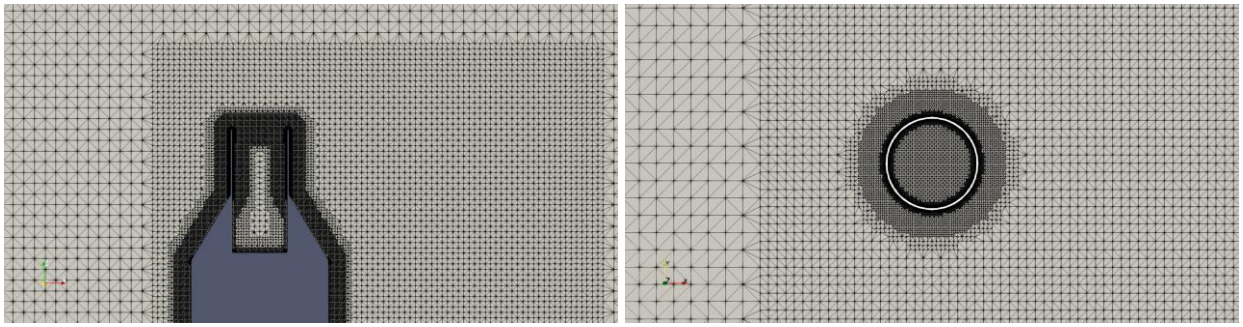

Figure 3 Refinement box around the *GeonorT200B*© gauge body and gradual refinement close to its surface in the central vertical section (x,z plane at y = 0, left-hand panel) and in the horizontal section at the gauge collector elevation (x,y plane at z = 0, right-hand panel) for simulations in both the uniform and turbulent free-stream conditions.

Finally, the two free-stream turbulence conditions were compared in terms of catch ratios and collection efficiency. The literature Lagrangian Particle Tracking model (*Colli e t al.*, 2015) was run upon the LES airflow fields for dry snow particles with equivalent diameters d = 0.25 - 0.5 - 0.75 mm and from 1 to 8 mm. In order to ensure the comparability between the two cases the airflow field in uniform free-stream conditions was scaled by assuming a reference wind speed equal to 2.5 ms^{-1} instead of 6 ms^{-1} as obtained for the turbulent free-stream condition downstream of the three columnar obstacles. The calculated catch ratios for each particle diameter are listed in Table 1. From the comparison, a stronger undercatch emerges for small size particles (less than 2mm) under turbulent free-stream conditions with respect to the uniform case, while the opposite occurs for larger particles (d > 2 mm). This is due to the higher attitude of the small size particles to follow the turbulent velocity fluctuations while larger particles are more inertial. Finally, the overall effect of the free stream turbulence on the collection performance of the gauge was quantified by computing the Collection Efficiency (CE) as the integral on the range of diameters after the introduction of the particle size distribution proposed by *Houze et al.* (1979). The calculated CE (Table 1) is higher in turbulent free-stream conditions. This result is in consistent agreement with the work of *Cauteruccio et al.* (2019), where the free-stream turbulence effect was investigated in terms of velocity and turbulence features of the airflow field, and moreover, demonstrates that the numerical derivation of correction curves for precipitation measurements as proposed in the literature under the simplifying assumption of uniform free-stream conditions is affected by a systematic overestimation of the wind-induced bias.

d [mm]	**0.25**	**0.5**	**0.75**	**1**	**2**	**3**	**4**	**5**	**6**	**7**	**8**	**CE**
Uniform	0.190	0.393	0.449	0.492	0.590	0.659	0.708	0.734	0.757	0.787	0.787	0.70
Turbulent	0.164	0.164	0.216	0.289	0.590	0.718	0.777	0.820	0.849	0.869	0.892	0.76

Table 1 Catch ratios obtained for each solid particle size and U_{ref} = 2.5 ms^{-1} using the LPT model and based on the LES airflow fields for the *GeonorT200B*© precipitation gauge in uniform and turbulent free-stream conditions and associated CE values.

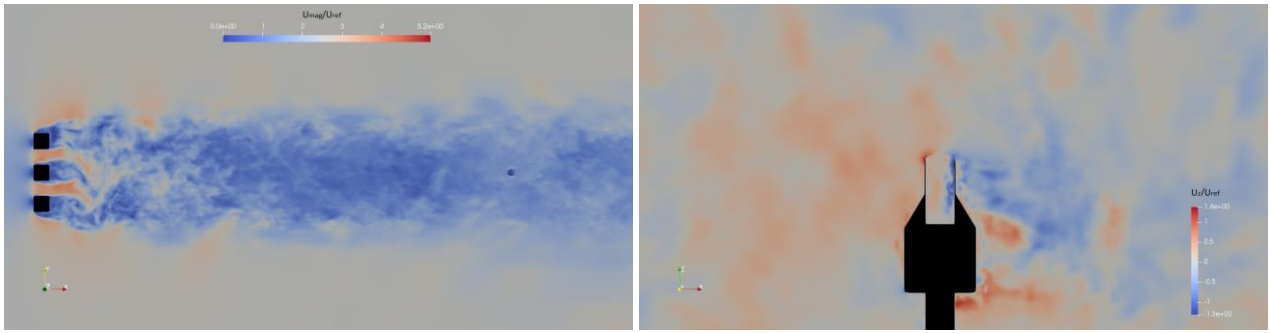

Figure 4 Normalized magnitude of the instantaneous flow velocity (U_{mag}/U_{ref}) in the horizontal plane (x,y) at the gauge collector elevation (z/D=0) (left-hand panel) and normalized vertical component (U_z/U_{ref}) of the instantaneous flow velocity in the vertical plane (x,z) at y/D=0 right-hand panel for the turbulent free-stream conditions.

REFERENCES

Cauteruccio A., Colli, M., Freda, A., Stagnaro, M. & Lanza, L.G. The role of the free-stream turbulence in attenuating the wind updraft above the collector of precipitation gauges. Journal of Atmospheric and Oceanic Technology, 2019, DOI:10.1175/JTECH-D-19-0089.1, (in press).

Colli, M., Lanza, L.G., Rasmussen, R., Thériault, J.M., Baker, B.C. & Kochendorfer, J. An improved trajectory model to evaluate the collection performance of snow gauges. Journal of Applied Meteorology and Climatology, 2015, 54, 1826–1836.

Colli, M., Pollock, M., Stagnaro, M., Lanza, L.G., Dutton, M. & O'Connell, P.E. A Computational Fluid-Dynamics assessment of the improved performance of aerodynamic raingauges. Water Resource Research, 2018, 54, 779–796.

Colli, M., Stagnaro, M., Theriault, J.M., Lanza, L.G. & Rasmussen, R. Adjustments for Wind-Induced Undercatch in Snowfall Measurements based on Precipitation Intensity. Journal of Hydrometeorology, 2019, (accepted).

Houze, R.A., Hobbs, P.V., Herzegh, P.H. & Parsons, D.B. Size distributions of precipitation particles in frontal clouds. Journal of the Atmospher Sciences, 1979, 36, 156–162.

Øistad, I.S. Analysis of the Turbulence Intensity at Skipheia Measurement Station, Master thesis, Norwegian University of Science and Technology, 2015.

Thériault, J.M., Rasmussen, R., Ikeda, K. & Landolt, S. Dependence of snow gauge collection efficiency on snowflake characteristics. Journal of Applied Meteorology and Climatology, 2012, 51, 745–762.